Optics & Laser Technology 78 (2016) 5–9

Contents lists available at ScienceDirect

Optics & Laser Technology

journal homepage: www.elsevier.com/locate/optlastec

Ultraviolet laser quantum well intermixing based prototyping of bandgap tuned heterostructures for the fabrication of superluminescent diodes

Romain Beal, Khalid Moumanis, Vincent Aimez, Jan J. Dubowski *

Interdisciplinary Institute for Technological Innovation (3IT), Department of Electrical and Computer Engineering, Université de Sherbrooke, 3000 boul. de l'Université, Sherbrooke, Québec, Canada J1K 0A3

ARTICLE INFO

Article history:
Received 15 June 2015
Received in revised form
20 September 2015
Accepted 3 October 2015

Keywords:
InGaAs/InGaAsP/InP quantum wells
Superluminescent diodes
Quantum well intermixing
Excimer laser processing

ABSTRACT

The ultraviolet laser induced quantum well intermixing process has been investigated for prototyping of multiple bandgap quantum well (QW) wafers designed for the fabrication of superluminescent diodes (SLDs). The process takes advantage of a krypton fluoride excimer laser (λ=248 nm) that by irradiating an InP layer capping GaInAs/GaInAsP QW heterostructure leads to the modification of its surface chemical composition and formation of point defects. A subsequent rapid thermal annealing step results in the selective area intermixing of the investigated heterostructures achieving a high quality bandgap tuned material for the fabrication of broad spectrum SLDs. The devices made from a 3-bandgap material are characterized by ~100 nm wide emission spectra with relatively flat profiles and emission exceeding 1 mW.

1. Introduction

Superluminescent diodes (SLDs) are broadband light sources employed in a variety of fiber based optical sensors [1], as well as for photonic testing system [2] and optical coherent tomography [3]. Typically, SLDs are made of epitaxially grown heterostructures comprising quantum wells (QW) or quantum dots (QD) designed for waveguiding optical signal, and with suppressed reflections at cavity ends for preventing the appearance of Fabry–Perot modes (unlike the cavity reflections in laser diode devices). The goal of an SLD device is to emit a bright signal with a large spectral width. The most common approach addressing this problem takes advantage of heterostructures with broad gain spectra achieved with multiple width QW architectures [4], large size distribution QD microstructures [5] or a combination of both QW and QD microstructures [6]. A relative advantage of QD over QW microstructures results from the significantly increased emission bandwidth of QD devices operating above a characteristic current density, where the emission from both excited and ground states becomes comparable and, thus, results in an enlarged output spectrum [7]. Alternative SLD architectures employ multiple structures emitting at different wavelengths and stacked along the waveguiding direction. Such architectures could be fabricated by the epitaxial growth techniques, but are less attractive due to a relatively complicated fabrication process [8,9]. Post-growth intermixing has also been investigated to increase spectral emission range of QW and QD wafers using impurity-induced intermixing [10], impurity-free vacancy diffusion intermixing [11,12] or infrared laser induced quantum well intermixing (QWI) [13].

Amongst the post-growth bandgap tuning techniques, ultraviolet laser induced QWI (UV-Laser-QWI) distinguishes itself as an attractive method of mask-free selective area processing with a significantly reduced risk of introducing extensive damage to the surface or sub-surface region of investigated microstructures. The irradiation of SiO_2 coated InP/InGaAs/InGaAsP QW microstructures, or direct irradiation in air and deionized water allows inducing significant bandgap blue shifts [14]. The experiments have revealed that laser irradiation in air leads to the formation of the InP_xO_y compound on the surface of a cap InP material, while irradiation in water leads to only a partially decomposed InP cap whose stoichiometry is restored following the rapid thermal annealing (RTA) step [15,16]. Consistent with these observations are relatively large bandgap blue shifts (~130 nm) found in microstructures processed in air with the excimer UV-Laser-QWI technique [15,17]. An example of the successful application of such an approach for device fabrication are high-intensity InGaAsP/InP laser diodes [18]. Recently, we have demonstrated that the UV-Laser-QWI process has the potential to deliver multi-bandgap

* Corresponding author.
E-mail addresses: romain.beal@usherbrooke.ca (R. Beal), khalid.moumanis@usherbrooke.ca (K. Moumanis), vincent.aimez@usherbrooke.ca (V. Aimez), jan.j.dubowski@usherbrooke.ca (J.J. Dubowski).

http://dx.doi.org/10.1016/j.optlastec.2015.10.002
0030-3992/

material with blue shifted amplitudes controlled to better than ± 8% [19], which may be attractive in exploring this technology for fabrication of commercial devices.

Here, we report on the successful use of the UV-Laser-QWI technique for fabrication of multi-bandgap wafers designed for the fabrication of broad spectrum SLDs. A comparative analysis of the performance of SLDs fabricated from the as-grown (unprocessed) material has revealed the attractive feature of the employed intermixing technique in achieving high-quality devices.

2. Experimental details

2.1. UV-laser-QWI

The experiments were carried out using a 5-QW InGaAs/InGaAsP/InP laser heterostructure designed to emit at 1.55 μm at room temperature. Fig. 1 shows a cross-section of the heterostructure capped with an undoped sacrificial layer of InP. The sacrificial layer is meant to be altered by the UV laser irradiation and removed at the end of the intermixing process by wet etching, leaving an undamaged wafer suitable for device fabrication. Two samples of the aforementioned heterostructure, referred to as A and B, were processed using a KrF excimer laser (Lumonics PM-848) based workstation equipped with a laser beam homogenization optics (MBX JPSA Sercel, Manchester, NH) [20]. The beam delivery system was designed to irradiate up to 15 mm × 15 mm masks that are imaged on the sample surface using a lens doublet with a 1.8 demagnification ratio. The samples were irradiated in an air environment with a 155 mJ/cm^2 pulse fluence of the laser operating at 2 Hz repetition rate. This resulted in changing the surface chemistry of the InP cap and creating an oxygen rich surface layer [15]. A bench top JIPELEC Jetfirst thermal processor was used to carry out RTA of the laser irradiated material. The samples were placed on a 4″ diameter silicon wafer whose temperature was monitored with a dedicated thermocouple. The annealing was performed in a forming gas environment of a 9:1 mixture of nitrogen and hydrogen. During the RTA step, the laser-induced point defects diffuse across the heterostructure and promote selective area intermixing of the QW and barrier species, which results in blue shifting of the sample bandgap energy. The blue shifting amplitude depends on the laser irradiation dose and RTA parameters [19]. A part of the sample A was irradiated with 60 pulses, while the remaining region of that sample was left unirradiated. In contrast, two regions of the sample B were irradiated with 15 and 60 pulses intended for the fabrication of a 3-bandgap material. The width of each irradiated region was defined at 625 μm using a step-and-repeat mask projection technique. Sample A was RTA for 2 min at 665 °C, while sample B was initially RTA for 2 min at 660 °C and, to increase the final intermixing amplitude, it was additionally RTA at 655 °C for 2 min. This corrective annealing was required due to the strong temperature dependence of PL blue shift, with a variation measured up to 1.8 nm/°C on a similar structure [19], and to the temperature measurement precision of the RTA processor limited to ± 5 °C. A 20 s long RTA ramp was necessary to heat the samples from room temperature to a set point temperature.

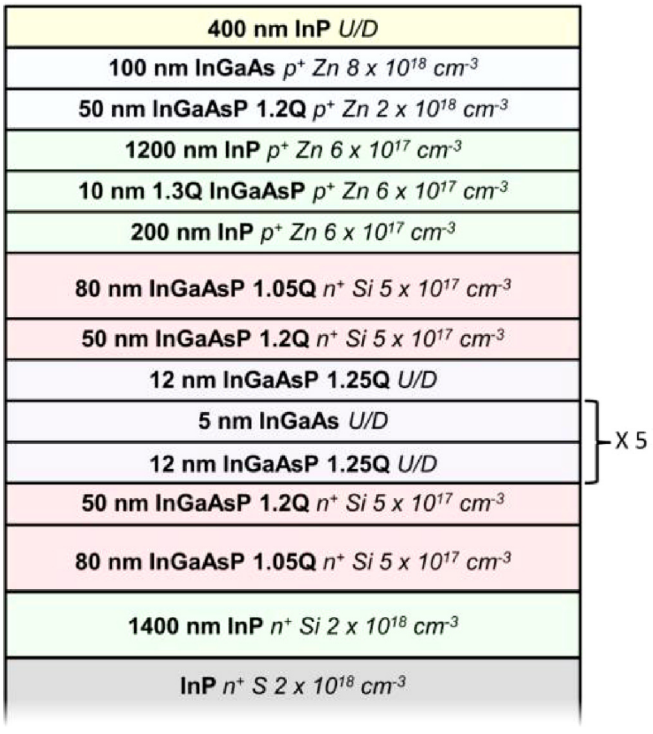

Fig. 1. Details of the 5-QW laser InGaAs/InGaAsP/InP heterostructure processed with the UV-Laser-QWI technique and employed for the fabrication of SLD devices.

The samples were characterized by collecting room temperature photoluminescence (PL) maps using a Philips PLM-150 system. Fig. 2 shows cross-section profiles of QW PL peak emission (λ_{PL}) measured across samples A (a) and B (b). It can be seen that sample A emits in the non-irradiated region at 1512 nm, while its emission has been blue shifted by 74 nm to 1438 nm in the laser processed region. The non-irradiated region of sample B emits at 1516 nm, its middle section emits at 1466 nm, while the most blue-shifted region, intended for the front section of an SLD device, emits 1428 nm. Thus, the maximum bandgap blue shift in both samples is almost identical, but as it will be illustrated in the next section, the presence of an additional blue-shifted section in sample B allows fabricating an SLD with a significantly stretched profile near its maximum emission intensity. It is of particular importance for the operation of devices fabricated from such a wafer that its PL peak intensity has not been affected by the intermixing process, and remained comparable in both irradiated and non-irradiated regions of the investigated samples. This result suggests that the QW heterostructure did not sustain a significant damage during the UV-Laser-QWI process, which is consistent with previously reported results [18].

2.2. Devices fabrication and test conditions

After PL characterization, broad area injection SLD were fabricated from samples A and B, and a reference device was fabricated from the as-grown material. Selective etching in an HCl:H_2O/1:1 solution for 6 min was applied to remove the sacrificial InP layer grown on InGaAs. Following this step, the samples were coated with a 200-nm-thick layer of silicon dioxide deposited with a plasma-enhanced chemical vapor deposition (PECVD) technique employing electronic grade source gases (SiH_4, N_2O and N_2 with a 99.999% purity). The thickness of this layer was verified by ellipsometry measurements. The current injection regions were opened in the dielectric by photolithography and wet etching using a buffered oxide etchant solution of NH_4F:HF/6:1 for 2 min. The injection regions were 30 μm wide, and tilted from the facet normal by 8° to prevent reflections in the cavity. Afterward, the top metal contact was deposited by evaporating a 70 nm thick layer of titanium and a 170 nm thick layer of gold. Mechanical thinning and polishing reduced the sample thickness down to 125 μm, and finally the back electrical contact was deposited by evaporating 14 nm of gold, 14 nm of germanium, 14 nm of gold, 11 nm of nickel and 200 nm of gold. All of the evaporation sources were of 99.999% purity, except for the nickel that was 99.995%

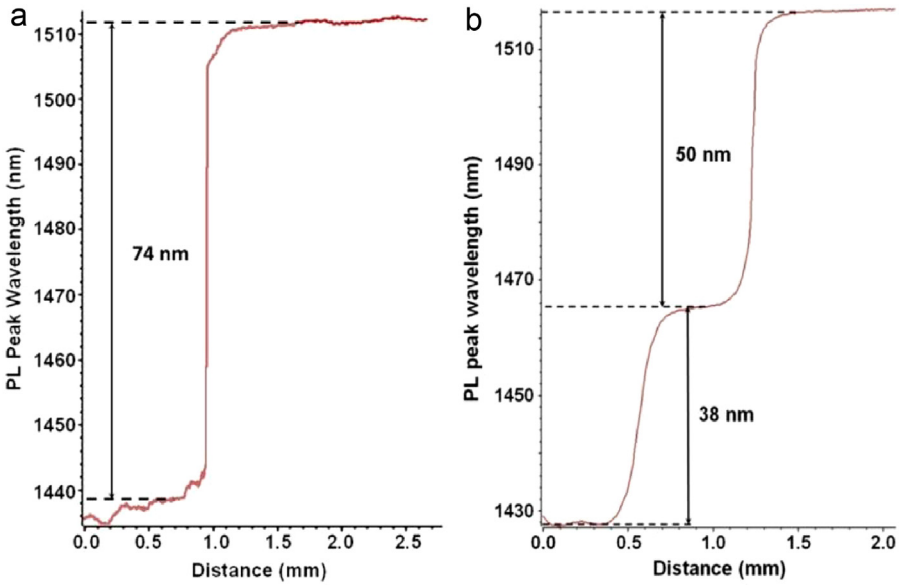

Fig. 2. PL peak wavelength profiles generated with the UV-Laser-QWI process across sample A (a) and B (b).

pure. A 1 min 400 °C annealing in nitrogen ensured the quality of the electrical contacts and completed the device fabrication process.

The devices were cleaved from the samples according to the blue shifted region positions at the desired device length. The sample A SLDs were cleaved to obtain 2.5 mm long devices with a 1.7 mm long rear non-irradiated region (λ_{PL}: 1512 nm) and a 0.8 mm long strongly intermixed front region (λ_{PL}: 1438 nm). For sample B, the active section was made 3 mm long. The lengths of the different bandgap energy sections were 700 μm for the front one (λ_{PL}: 1428 nm), 600 μm for the middle one (λ_{PL}: 1466 nm), and 1700 μm for the rear section (λ_{PL}: 1516 nm). The shorter total length of the sample A devices was meant to limit gain narrowing and therefore the intensity drop between the signal contributions of the two bandgap regions. The sample B SLDs included an additional 600 μm long non-pumped non-intermixed absorption region. This was designed to limit reflections in the cavity of the 3 mm long active region device. An extended length waveguide microstructure of the SLD device is expected to deliver a larger total gain and therefore increased output power, but it is consequently more sensitive to parasitic reflections resulting in the apparition of lasing modes in the output spectrum.

After fabrication, the diodes were tested under pulsed current condition using a Keithley 2520 laser diode test setup. The pulse width was limited to 2.5 μs with a 1 ms delay between each pulse. This duty cycle was chosen to prevent Joule heating that would have altered devices performances at high-injected current value, while remaining in the current generator and photodetector operational limitations for pulse duration. A Newport 1830C photodiode was used to measure the light – intensity characteristics of SLD devices. The SLD signal was coupled into a multimode 62.5 μm diameter core fiber, allowing collecting spectra with an Optical Spectrum Analyzer (OSA) Agilent 86140B.

3. Results and discussion

3.1. Sample A devices

The analysis of SLD devices revealed, as expected, a strong dependence of their output spectra on the injected current. The broadest spectrum of an SLD device made from sample A is shown in Fig. 3. Its full width at half maximum (FWHM) of 124 nm has been achieved with the injection current of 1.3 A. Two clearly distinguished peaks, centered near 1450 nm and 1520 nm, can be observed in that case. The peaks are separated by an approximately 70-nm wide region of a reduced by up to 40% emission intensity. It is clear that the overlapping of the emission spectra of the 2-bandgap material of sample A was insufficient to achieve a broad range emission spectrum with a flat top profile. For current values below 1.3 A, the 1450 nm peak dominated the entire spectrum, while for greater currents, it was the 1520 nm peak emission that contributed the most to the spectrum. Also, the lasing modes visible near the 1520 nm peak indicate a limited efficiency of the device in suppressing lateral modes within the cavity.

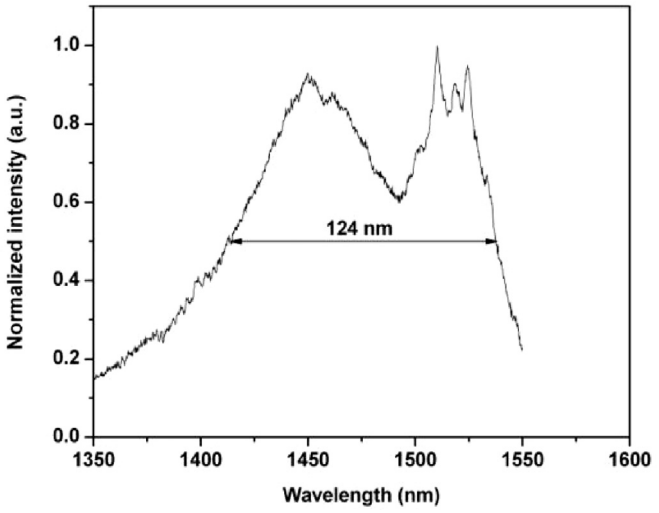

Fig. 3. Broadband emission spectrum of an SLD device fabricated from sample A.

The power emitted by this device at the injection current of 1.3 A was of 0.65 mW, which is comparable to the power emitted by the reference device.

3.2. Sample B devices

Fig. 4 shows current dependent emission spectra of an SLD device fabricated from the sample B material. It can be seen that at

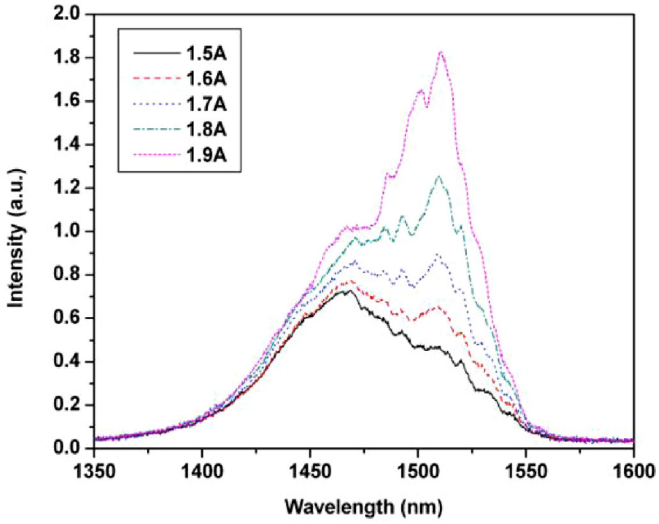

Fig. 4. Evolution of emission spectra in an SLD device fabricated in sample B for injected currents ranging from 1.5 to 1.9 A.

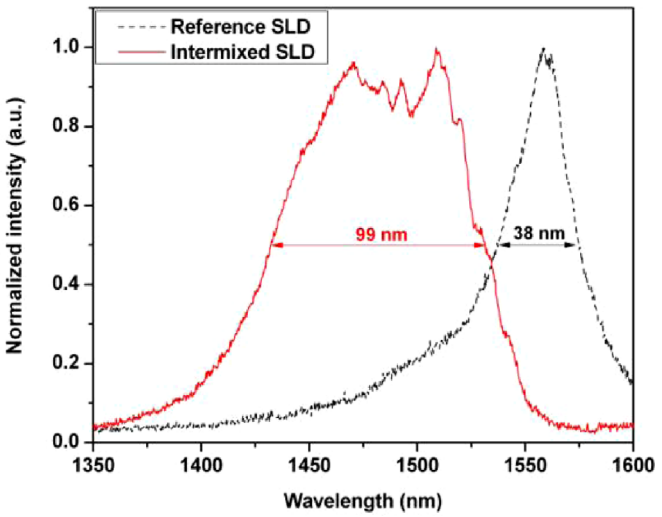

Fig. 5. Emission spectra from SLD devices fabricated in sample B (Intermixed SLD) and in as-grown non-irradiated non-annealed material (Reference SLD). The output power emitted in both cases is 1.1 mW.

1.5 and 1.6 A, the spectra are dominated by emission centered at 1465 nm that originates from the QWI material. In contrast, the spectra generated with currents of 1.8 and 1.9 A are dominated by emission centered at 1510 nm that originates from the non-intermixed material. The optimum shape spectrum, centered around 1480 nm, has been observed for a driving current of 1.7 A. Variations of SLD spectra as a function of current have commonly been observed for broad spectrum sources based on QD [21] or asymmetric QW SLD [22] microstructures, for which the heterostructure gain spectra are strongly related to carrier density. In our case, for both samples A and B the SLD device spectral dependence on the injected current can be predominantly attributed to the competition between the signals from the rear and front sections. For low current densities, the low-energy photons from the rear section of the device are also attenuated while traveling through the intermixed front region. Therefore the contribution to the output signal comes mostly from the front intermixed section. As the current increased, the signal intensity from the longer rear region increased faster than the signal from the front section and became prominent for current exceeding an equilibrium value of 1.3 A for sample A SLDs and 1.7 A for sample B SLDs.

In Fig. 5, we compare the sample B SLD spectrum at 1.7 A with the spectrum of a device fabricated from a non-intermixed material at equivalent output power of 1.1 mW. It can be seen that the architecture of an SLD device based on a 3-band gap material allowed increasing the width of an emitted spectrum by 2.5 times (FWHM ≈ 100 nm) in comparison to the spectrum emitted by a device fabricated from a non-intermixed material (FWHM ≈ 40 nm). The insertion of a middle section, blue shifted by 50 nm in comparison to the rear section emission, resulted in the disappearance of the aforementioned intensity drop in the middle of the SLD emission spectrum. However, the FWHM of the spectrum emitted by this device is 25 nm narrower in comparison to that of the device made from the sample A material. Several phenomena may be responsible for this behavior. Firstly, the increased device length from 2.5 mm to 3 mm is expected to result in a slightly increased gain of this device, which could lead to gain narrowing of the emitted spectrum [23]. Secondly, a shorter wavelength portion of the signal emitted from the rear section is likely amplified preferentially while traveling through the middle section, hence resulting in its narrowing. This can be explained by considering the steady state traveling wave rate equation describing the photon density variation in the forward direction z of the cavity [24,25]:

$$\partial S(\lambda, z)/\partial z = (g(\lambda, z) - \alpha(\lambda, z))\cdot S(\lambda, z) + \beta_{SP}\cdot R_{SP}(\lambda, z),$$

where S denotes the photon density, g the modal gain, α the internal loss, β_{SP} the spontaneous emission coupling coefficient, and $R_{SP}(\lambda,z)$ the spontaneous emission rate. The first term on the right hand side shows that the signal variation along z is linked to the gain value at the z position. Since the gain spectrum varies along the waveguiding direction in the intermixed material [26], the rear section spectrum is expected to be altered by the blue shifted heterostructure in front of it. In the sample A device, the front section is blue shifted by 74 nm with respect to the rear section, thus the overlapping of its gain spectrum with the signal from the rear section is relatively weaker than the overlapping in the sample B device. Nevertheless, the results for both samples discussed in this report can be favorably compared to those obtained for a device with a bandgap energy gradient profile [13] where the gradually changing gain spectrum included also a signal originating from a significantly blue shifted front part of the device.

The light-current plots of the devices discussed in Fig. 5 are shown in Fig. 6. They indicate that at currents of up to approximately 1.5 A the output power of these devices is practically identical, and equal to 0.5 mW at 1.5 A. For currents greater than 1.5 A, the power of the intermixed SLD increases slower with the current than that of the reference device. This result is quite anticipated given that the reference device was made of a single bandgap energy material having the same gain spectrum along the waveguide where light amplification is expected to be more efficient.

These results demonstrate attractive features of the UV-Laser-QWI technique employed for convenient fabrication of multibandgap material from a single bandgap QW wafers. The process control and the ability to yield a low-defect material made it possible to fabricate SLD devices of relatively high emission power from a 3-bandgap material. It seems feasible that optimization of this approach, including advanced device modeling should lead to the fabrication of further advanced SLD and related multi-bandgap devices.

4. Conclusion

We have investigated the UV-Laser-QWI technique for post-processing of GaInAs/GaInAsP QW wafers and fabrication of broad-spectrum SLD devices.

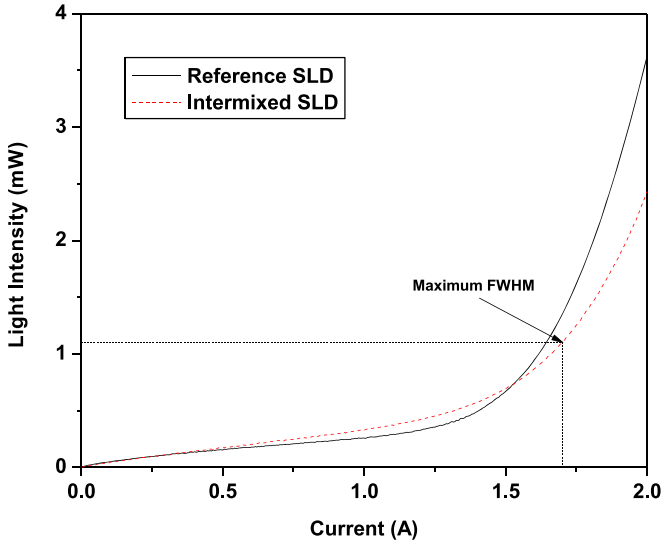

Fig. 6. Light-Intensity characteristics of SLD devices fabricated from the intermixed (dashed line) and as-grown (solid line) material of sample B.

- The ability to produce different multi-bandgap material by adjusting the laser dose delivered to the wafer was employed for direct (without a photolithographic step) prototyping of two different wafer heterostructures.
- The light-current (LI) characteristics of the intermixed SLDs devices was found to be relatively close to this of the reference (fabricated from the non-intermixed material) devices, confirming that the UV-Laser-QWI process does not degrade significantly the optical characteristics of the as-grown heterostructures.
- The superluminescent devices, produced from a 2-bandgap and a 3-bandgap material, yielded broadband emission of FWHM equal to ~125 nm and ~100 nm, respectively. The related output power of these devices was 0.65 mW and 1.1 mW, respectively, although non-optimized emission exceeding 2 mW was easily achievable with devices made from a 3-bandgap material.

The fabrication of a 3-bandgap material discussed in this report illustrates an attractive application of the UV-Laser-QWI technique for prototyping of QW wafers useful for the fabrication of SLDs devices with enhanced parameters. It seems feasible that further optimization of this approach, including advanced device modeling should lead to the fabrication of SLDs and other multi-bandgap devices at attractive cost for applications in photonic sensing and wide range diagnostics.

Acknowledgments

This research was supported by the Canada Research Chair in Quantum Semiconductors Program (NSERC No. 950-220304), NanoQuébec and Le Fonds Québécois de la Recherche sur la Nature et les Technologies. Semiconductor wafers, whose acquisition was partially supported by CMC Microsystems (Kingston, Ontario), were grown at the Canadian Photonics Fabrication Center (Ottawa, Canada). The authors would like to thank the staff of the Université de Sherbrooke Interdisciplinary Institute for Technological Innovation (3IT) for providing technical support.

References

[1] M.G. Vasilyev, V.K. Sacharov, A.A. Shelyakin, A fiber-optic open-path methane sensor, Laser Phys. 9 (1999) 940–942.
[2] Y. Liu, Passive Components Tested by Superluminescent Diodes, WDM Solut, 2000, pp. 41–41.
[3] L. Carrion, M. Lestrade, Z. Xu, G. Touma, R. Maciejko, M. Bertrand, Comparative study of optical sources in the near infrared for optical coherence tomography applications, J. Biomed. Opt. 12 (2007) 014017.
[4] C.-F. Lin, B.-L. Lee, Extremely broadband AlGaAs/GaAs superluminescent diodes, Appl. Phys. Lett. 71 (1997) 1598.
[5] S. Haffouz, P.J. Barrios, R. Normandin, D. Poitras, Z. Lu, Ultrawide-bandwidth, superluminescent light-emitting diodes using InAs quantum dots of tuned height, Opt. Lett. 37 (2012) 1103–1105.
[6] S. Chen, K. Zhou, Z. Zhang, J.R. Orchard, D.T.D. Childs, M. Hugues, O. Wada, R. A. Hogg, Hybrid quantum well/quantum dot structure for broad spectral bandwidth emitters, IEEE J. Sel. Top. Quantum Electron. 19 (2013).
[7] M.Z.M. Khan, H.H. Alhashim, T.K. Ng, B.S. Ooi, High-power and high-efficiency 1.3-μm superluminescent diode with flat-top and ultrawide emission bandwidth, IEEE Photonics J. 7 (2015) 1–8.
[8] Y. Kashima, T. Munakata, Broad spectrum InGaAsP edge-emitting light-emitting diode using selective-area metal-organic vapor-phase epitaxy, IEEE Photonics Technol. Lett. 10 (1998) 1223–1225.
[9] N. Ozaki, K. Takeuchi, S. Ohkouchi, N. Ikeda, Y. Sugimoto, H. Oda, K. Asakawa, R. A. Hogg, Monolithically grown multi-color InAs quantum dots as a spectral-shape-controllable near-infrared broadband light source, Appl. Phys. Lett. 103 (2013) 051121–051124.
[10] T.-K. Ong, M. Yin, Z. Yu, Y.-C. Chan, Y.-L. Lam, High performance quantum well intermixed superluminescent diodes, Meas. Sci. Technol. 15 (2004) 1591–1595.
[11] C.D. Xu, G.T. Du, J.F. Song, Y.Z. Huang, Enhancement of the spectral width of high-power 1.5 μm integrated superluminescent light source by quantum well intermixing process, Chin. Phys. Lett. 21 (2004) 963–965.
[12] K.J. Zhou, Q. Jiang, Z.Y. Zhang, S.M. Chen, H.Y. Liu, Z.H. Lu, K. Kennedy, S. J. Matcher, R.A. Hogg, Quantum dot selective area intermixing for broadband light sources, Opt. Express 20 (2012) 26950–26957.
[13] R. Beal, K. Moumanis, V. Aimez, J.J. Dubowski, Enhanced spectrum superluminescent diodes fabricated by infrared laser rapid thermal annealing, Opt. Laser Technol. 54 (2013) 401–406.
[14] J. Genest, R. Beal, V. Aimez, J.J. Dubowski, ArF laser-based quantum well intermixing in InGaAs/InGaAsP heterostructures, Appl. Phys. Lett. 93 (2008) 071106.
[15] N. Liu, J.J. Dubowski, Chemical evolution of InP/InGaAs/InGaAsP microstructures irradiated in air and deionized water with ArF and KrF lasers, Appl. Surf. Sci. 270 (2013) 16–24.
[16] N. Liu, S. Poulin, J.J. Dubowski, Enhanced photoluminescence emission from bandgap shifted InGaAs/InGaAsP/InP microstructures processed with UV laser quantum well intermixing, J. Phys. D: Appl. Phys. 46 (2013) 445103.
[17] M. Kaleem, X. Zhang, Y. Zhuang, J.-J. He, N. Liu, J.J. Dubowski, UV laser induced selective-area bandgap engineering for fabrication of InGaAsP/InP laser devices, Opt. Laser Technol. 51 (2013) 36–42.
[18] M. Kaleem, X. Zhang, Y.-g Yang, Y. Zhuang, J.-j He, Multi-bandgap photonic materials and devices fabricated by UV-laser induced quantum well intermixing, Optoelectron. Lett. 9 (2013) 358–361.
[19] R. Beal, V. Aimez, J.J. Dubowski, Excimer laser induced quantum well intermixing: a reproducibility study of the process for fabrication of photonic integrated devices, Opt. Express 23 (2015) 1073–1080.
[20] K. Mann, Laser beam characterization, in: D. Basting, G. Marowsky (Eds.), Excimer Laser Technology, Springer, Berlin Heidelberg, 2005, pp. 105–117.
[21] I. Han, H.D. Chang, J.D. Song, J.-I. Lee, J.I. Lee, Study on superluminescent diodes using InGaAs–InAs chirped quantum dots, J. Korean Phys. Soc. 45 (2004) 1193–1195.
[22] J. Wang, M.J. Hamp, D.T. Cassidy, Design considerations for asymmetric multiple quantum well broad spectral width superluminescent diodes, IEEE J. Quantum Electron. 44 (2008) 1256–1262.
[23] M. Loeser, L. Occhi, C. Vélez, R. Rezzonico, B. Witzigmann, Performance analysis of 1300 nm SLEDs-impact of temperature and length scaling, Opt. Quant Electron. 38 (2006) 1069–1075.
[24] M. Loeser, B. Witzigmann, Multidimensional electro-opto-thermal modeling of broad-band optical devices, IEEE J. Quantum Electron. 44 (2008) 505–514.
[25] N. Matuschek, M. Duelk, Modeling and simulation of superluminescent light-emitting diodes (SLEDs), IEEE J. Sel. Top. Quantum Electron. 19 (2013).
[26] H. Li, Semiconductor Quantum Wells Intermixing, Gordon and Breach Science Publishers, 2000.